High blood pressure arising from a defect in vascular function

Simon K. Michael*, Howard K. Surks*, Yuepeng Wang*, Yan Zhu*, Robert Blanton*, Michelle Jamnongjit*, Mark Aronovitz*, Wendy Baur*, Kenichi Ohtani*, Michael K. Wilkerson†, Adrian D. Bonev†, Mark T. Nelson†, Richard H. Karas*, and Michael E. Mendelsohn*‡

*Molecular Cardiology Research Institute, Tufts Medical Center, Tufts University School of Medicine, Boston, MA 02111; and †Department of Pharmacology, University of Vermont, Burlington, VT 05405

Communicated by David E. Housman, Massachusetts Institute of Technology, Cambridge, MA, March 8, 2008 (received for review January 20, 2008)

Hypertension, a major cardiovascular risk factor and cause of mortality worldwide, is thought to arise from primary renal abnormalities. However, the etiology of most cases of hypertension remains unexplained. Vascular tone, an important determinant of blood pressure, is regulated by nitric oxide, which causes vascular relaxation by increasing intracellular cGMP and activating cGMP-dependent protein kinase I (PKGI). Here we show that mice with a selective mutation in the N-terminal protein interaction domain of PKGIα display inherited vascular smooth muscle cell abnormalities of contraction, abnormal relaxation of large and resistance blood vessels, and increased systemic blood pressure. Renal function studies and responses to changes in dietary sodium in the PKGIα mutant mice are normal. These data reveal that PKGIα is required for normal VSMC physiology and support the idea that high blood pressure can arise from a primary abnormality of vascular smooth muscle cell contractile regulation, suggesting a new approach to the diagnosis and therapy of hypertension and cardiovascular diseases.

cyclic nucleotides | hypertension | nitric oxide | vascular biology | vascular smooth muscle

Elevated blood pressure is a major risk factor for cardiovascular diseases and is responsible for widespread morbidity and mortality (1). Blood pressure is regulated by a variety of complex neurohumoral and mechanical signals that together determine systemic vascular tone and resistance (2, 3). The prevailing model for elevated blood pressure states that renal abnormalities of sodium handling cause volume expansion, increased systemic vascular resistance, and hypertension, and a large number of physiologic and genetic studies support this model and the central role of the renal renin–angiotensin–aldosterone system in blood pressure regulation (4–8). Changes in vascular morphology and tone can increase vascular resistance and blood pressure (5), but the hypothesis that primary abnormalities of vascular smooth muscle tone can cause hypertension has not been sufficiently tested (6).

Vascular smooth muscle contraction is initiated by both calcium-dependent and -independent mechanisms. Increases in intracellular calcium from receptor- or ion channel-activated pathways (2) lead to activation of myosin light chain kinase, which phosphorylates myosin light chains, activating myosin ATPase and increasing vascular smooth muscle cell (VSMC) contraction and vascular tone. The central calcium-independent pathway regulating VSMC tension is mediated by the GTPase RhoA and Rho kinase, which promote VSMC differentiation, stress fiber formation, and contraction, also increasing vascular tone (2, 7). Conversely, VSMC relaxation is mediated by activation of myosin light chain phosphatase (MLCP), which dephosphorylates myosin light chains to cause relaxation. The relative proportion of phosphorylated and dephosphorylated myosin light chains thus determines the state of VSMC tone (reviewed in ref. 2). Nitric oxide, the most important endogenous vasodilator, causes VSMC relaxation by increasing intracellular cGMP and activating PKGI (reviewed in refs. 9 and 10).

The two known mammalian cGMP-dependent protein kinases, PKGI and PKGII, are encoded by distinct genes. PKGI is expressed in vascular and all smooth muscle cells, as well as platelets, the central nervous system, and renal mesangial and interstitial myofibroblasts, but not in renal parenchymal cells (11, 12), whereas PKGII is expressed in the brain, intestinal mucosa, chondrocytes, lung, renal parenchyma, and the renal renin-secreting cells and adrenal zona glomerulosa cells. PKGII but not PKGI inhibits renin secretion by the kidney (13, 14) and regulates basal aldosterone production by the adrenal gland (15). PKGI mediates vascular relaxation by endothelial-derived nitric oxide and related nitrovasodilators (10, 16) (*SI Text*) both by activating MLCP (17) and by inhibiting the Rho/Rho kinase contractile pathway (18–21). The PKGI gene encodes two isoforms, PKGIα and PKGIβ, which are identical except for their N termini, which are encoded by alternative splicing of distinct first exons to the remaining exons of the PKGI gene, and include leucine zipper (LZ) heptad repeat motifs critical for protein targeting (22). Mice in which the PKGI gene is inactivated in the germ line lack both PKGI isoforms throughout ontogeny. These mice are terminally ill when born (the majority die before 6 weeks of age) and have multiple cardiovascular, gastrointestinal, hematopoietic, and neurological defects that preclude complete investigation of most cardiovascular functions, including blood pressure (13, 23). PKGIα and PKGIβ both regulate VSMC tone through interactions with key VSMC contractile proteins mediated by their respective LZ domains (10, 16, 17, 24). PKGIα promotes vascular relaxation by regulation of the two major VSMC pathways regulating contractile state. We have previously shown that PGKIα binds to MLCP specifically via a LZ domain-mediated interaction that is required for activation of MLCP, causing myosin light chain dephosphorylation and relaxation (17). PKGIα also phosphorylates RhoA on serine-118, which inhibits Rho/Rho kinase-induced VSMC stress fiber formation and contraction (20, 21).

Results

To determine the *in vivo* importance of PKGIα targeting to the key VSMC protein complex regulating contraction, we gener-

Author contributions: S.K.M., and H.K.S. contributed equally to this work; S.K.M., H.K.S., M.K.W., A.D.B., M.T.N., R.H.K., and M.E.M. designed research; S.K.M., H.K.S., Y.W., Y.Z., R.B., M.J., M.A., W.B., K.O., M.K.W., A.D.B., M.T.N., R.H.K., and M.E.M. performed research; H.K.S., Y.W., Y.Z., R.B., M.A., and M.T.N. contributed new reagents/analytic tools; S.K.M., H.K.S., Y.Z., R.B., M.J., M.T.N., R.H.K., and M.E.M. analyzed data; and H.K.S., R.H.K. and M.E.M. wrote the paper.

The authors declare no conflict of interest.

‡To whom correspondence should be addressed. E-mail: mmendelsohn@tuftsmedicalcenter.org.

This article contains supporting information online at www.pnas.org/cgi/content/full/0802128105/DCSupplemental.

ated knockin mice harboring a discrete mutation in PKGIα that disrupts the LZ domain essential for PKGIα-mediated regulation of VSMC myosin phosphatase and relaxation. The initial four LZ leucine/isoleucine codons in exon 1α of the endogenous PKGIα allele were replaced by alanines [supporting information (SI) Fig. S1] to yield leucine zipper mutant (LZM) mice that express mutant PKGIα protein with an LZ incapable of binding to MLCP (17, 25), but with otherwise identical sequence to WT PKGI (26). In contrast to mice with germ-line inactivation of the PKGI gene (23), homozygous mutant LZM PKGIα mice are viable, appear grossly normal, are born in a normal Mendelian distribution, and feed, grow, and age normally (Table S1 and *SI Text*). LZM PKGIα mouse blood vessels express levels of LZ mutant PKGIα protein similar to PKGIα in the WT mice, and neither total PKGI expression nor PKGIβ expression is significantly altered in blood vessels or other tissues from WT and mutant mice (*SI Text*, Fig. 1*A* and Figs. S2 and S3 *A* and *B*). Mutant PKGIα protein in VSMC remains responsive to cGMP, with a maximal cGMP-stimulated activity similar to WT PKGI (Fig. 1*B*). PKGIα targeting and activation of MLCP causes myosin light chain dephosphorylation and relaxation (17), and as expected, the direct interaction between PKGIα and myosin phosphatase mediating this pathway is fully disrupted in the LZ mutant PKGIα (Fig. 1*C* and *SI Text*). PKGI phosphorylates RhoA on serine-118, which inhibits the Rho/Rho kinase contractile pathway (20, 21). RhoA S188-PO_4 was markedly reduced in the LZM VSMC (Fig. 1*D*), and Rho activity assays (*SI Text*) from WT and LZM VSMC showed a 6-fold increase in Rho activity in the LZM PKGIα cells (Fig. 1*E*). These data demonstrate that LZ-mediated targeting is critical for PKGIα-mediated inhibition of RhoA and confirm *in vivo* the importance of PKGIα regulation of the Rho/Rho kinase pathway (20, 21) in normal VSMC.

Freshly dispersed, unstimulated VSMC from WT and LZM mouse arteries are the same size, as determined by direct electrophysiological measures of cellular capacitance (WT = 12.3 ± 0.9 pF, LZM = 11.9 ± 1.0 pF, $n = 7$, not statistically significant (*SI Text* and Fig. 2*A*), and whole-cell potassium currents from LZM and WT cells also are similar (*SI Text* and Fig. S4*A*). These sensitive capacitance measurements of freshly dispersed, unstimulated VSMC show that the sizes of WT and LZM VSMCs are not different. Stimulation of freshly dispersed WT and LZM VSMC with serum in culture conditions caused marked increases in stress fiber formation in the LZM cells [17.7 ± 1.9 (WT) vs. 61.7 ± 6.9 (LZM) stress fibers per VSMC (mean ± SD), $n = 15$–17, $P < 0.0001$] (*SI Text* and Fig. 2 *B* and *C*), which adopted a broader, spread morphology compared with WT cells due to stimulation [mean cell size: WT, 846 ± 73 μm^2 ($n = 20$); LZM, 2,005 ± 158.7 m^2 ($n = 16$), $P < 0.001$]. Similar results were obtained for cells obtained by either the explant method (*SI Text*, Fig. 2*B*, and Fig. S4*B*) or enzymatic dispersion (Fig. S4*C*), and these responses were retained for at least 10–12 cell passages. This VSMC phenotype is characteristic of that seen in cells expressing constitutively active forms of RhoA (19, 27) and is consistent with the biochemical assays of Rho phosphorylation and function (Fig. 1 *D* and *E*). Immunofluorescence studies confirmed little or no detectable PKGIα-phosphorylated RhoA (RhoA-188S-PO4) in the LZM VSMC (Fig. 2*B*). VSMC differentiation to the contractile phenotype is characterized by actin polymerization, stress fiber formation, and expression of smooth muscle-specific genes, a process also regulated by RhoA/Rho kinase activation (2, 7). Expression of smooth muscle-specific genes, including myosin heavy chain, smooth muscle α-actin, smoothelin, and calponin, was significantly increased in LZM VSMC in comparison with WT cells (Fig. 2*D*). Taken together, these data support that vascular smooth muscle cells from LZM mice have loss of PKGIα-mediated RhoA/Rho kinase inhibition and constitutive activation of the Rho/Rho kinase contractile pathway.

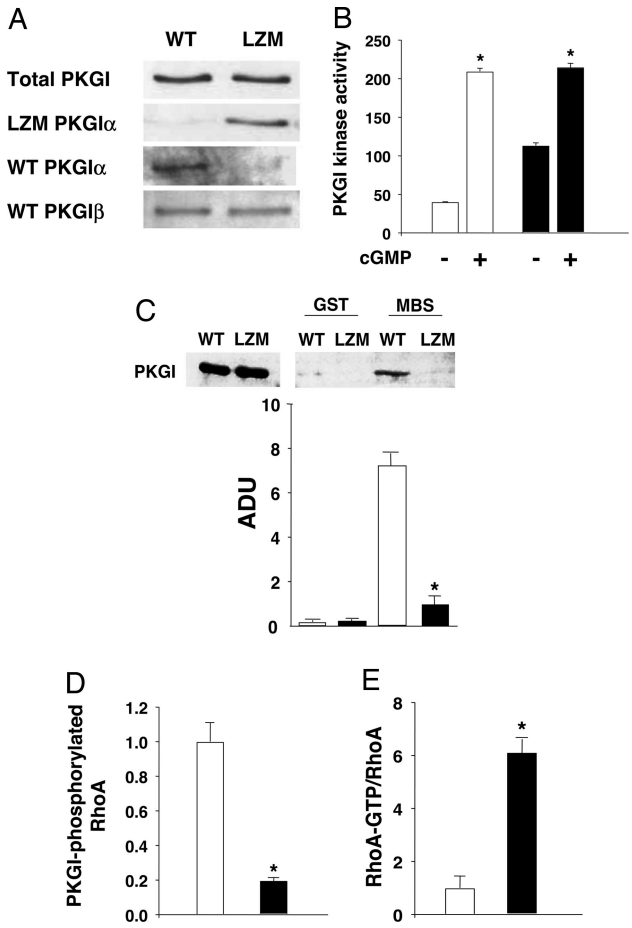

Fig. 1. PKGI expression and function and RhoA regulation in VSMC from WT and LZM mice. (*A*) LZM blood vessels express LZM-PKG protein but not WT PGKIα. Immunoblots of aortic lysates from WT and LZM mice with antibodies recognizing all forms of total PKGI or specific for WT PKGIα, WT PKGIβ, or PKGI LZM protein. Total PKGI and PGKIβ expression levels were unchanged by the presence of the targeted mutation ($n = 3$, not statistically significant) (Fig. S3 *A* and *B*). (*B*) WT and LZM PKGIα cGMP-dependent kinase activity. cGMP-inducible PKGI activity (femtomoles of PO_4 per minute per microgram of protein) measured in WT and LZM cell lysates from aortic smooth muscle using the PKGI-specific substrate BPDEtide. Inducible kinase activity was the same in LZM and WT extracts (*, $P < 0.05$ vs. unstimulated kinase; not statistically significant, WT maximal vs. LZM maximal; one of three similar experiments is shown). White bars, WT activity; black bars, LZM activity. (*C*) Loss of PKGIα–myosin binding subunit (MBS) interaction in PKGIα LZM mouse VSMC. Binding of PKGI from WT and LZM VSMC lysates to MBS was tested by using GST fusion protein pull-down experiments. PKGIα from LZM VSMC failed to interact with GST-MBS, whereas WT PKGIα bound MBS as expected and reported previously (17). White bars, WT PKG; black bars, LZM PKG. ADU, arbitrary densitometric units ($n = 3$; *, $P < 0.001$ vs. WT). Two percent lysate input is shown (*Left*). (*D*) PKGI-mediated Rho phosphorylation in WT and LZM VSMC. Levels of RhoA S188-PO_4, normalized for total RhoA, were measured in WT and LZM VSMC by immunoblotting with phosphospecific antibody and quantified by densitometry. PKG LZM lysate had an 80% reduction in RhoA S188-PO_4 compared with PKG WT lysate ($n = 3$; *, $P < 0.01$ vs. WT). White bar, WT; black bar, LZM. (*E*) RhoA activation is increased in LZM VSMCs. RhoA activation was measured by binding of RhoA from WT and LZM VSMC lysates to GST-Rhotekin (34). LZM RhoA-GTP was increased 6-fold compared with WT RhoA-GTP ($n = 3$, $P < 0.01$). White bar, WT; black bar, LZM.

The regulation of vasomotor tone in both large and resistance vessels was studied. Aortic rings from PKGIα LZM mice were morphologically normal but demonstrated impaired nitric oxide-

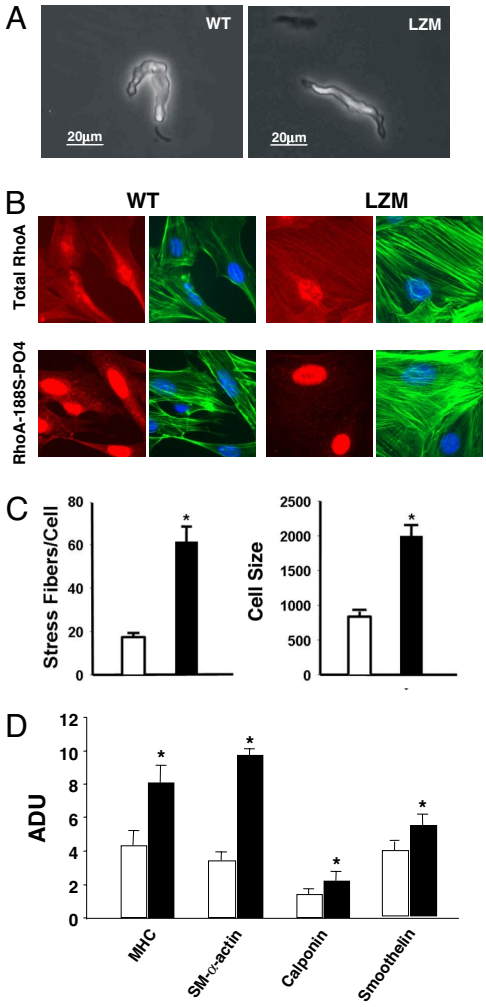

Fig. 2. Characterization of VSMC in WT and LZM mice. (*A*) Phase contrast microscopy of typical freshly dispersed, unstimulated WT (*Left*) and LZM (*Right*) arterial VSMC used to measure capacitance (*SI Text*). (*B*) Stress fiber formation and cGMP-mediated RhoA phosphorylation in WT and LZM VSMC. Serum-stimulated isolated aortic VSMCs from WT and LZM mice are shown. Shown is immunofluorescence staining of total RhoA (*Upper*) or PKGI-phosphorylated RhoA (*Lower*) with rhodamine-conjugated total RhoA or RhoA-S188-PO_4 antibodies, respectively (red), and actinomyosin stress fibers stained with phalloidin (green). DAPI-stained nuclei are shown in blue. (*C*) Stress fiber content and cell size in serum-stimulated WT and LZM VSMC. Phalloidin-stained stress fibers were counted microscopically, and cell size was determined by computerized morphometric cell area measurements ($n = 20$; *, $P < 0.0001$ for stress fibers per cell and $P < 0.001$ for cell size). White bars, WT; black bars, LZM. (*D*) Expression of smooth muscle-specific proteins in serum-stimulated WT and LZM VSMC. Expression of all VSMC-specific proteins shown was increased in LZM VSMC. MHC, myosin heavy chain, SM-α actin, smooth muscle α-actin. $n = 3$; *, $P < 0.05$ vs. WT. White bars, WT; black bars, LZM. ADU, arbitrary densitometric units.

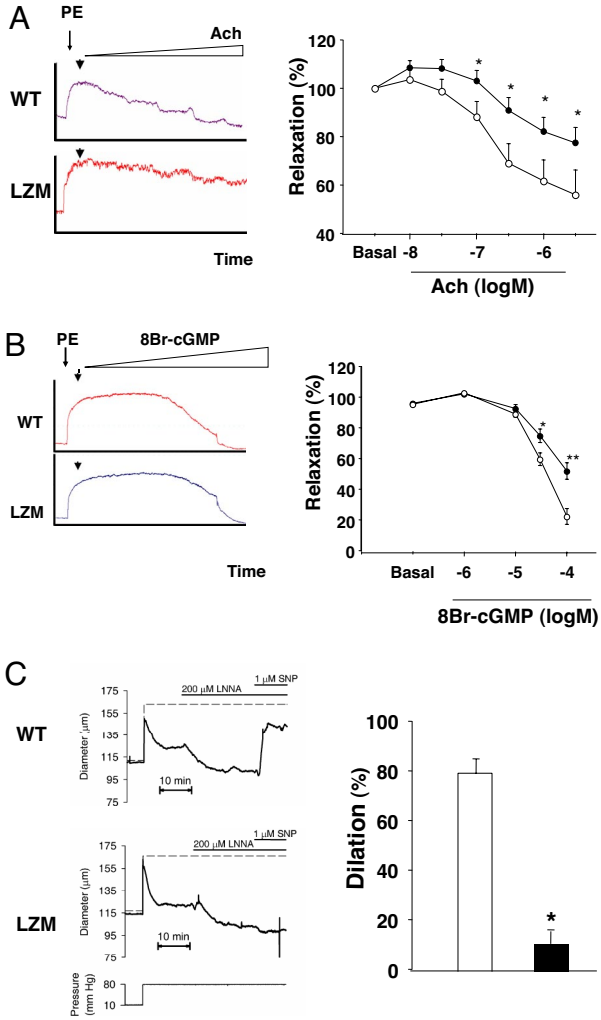

Fig. 3. Vasomotor function of large and resistance arteries from LZM and WT mice. (*A* and *B*) Studies of vascular aortic rings from WT and LZM mice. Significantly impaired relaxation was noted in LZM aortic rings to both the endothelium-dependent vasodilator acetylcholine (Ach) (*A*) and the direct VSMC relaxant 8-bromo-cGMP (8Br-cGMP), a nonhydrolyzable analogue of cGMP (*B*). Single tracings are shown for WT and LZM rings in *Left*, and summary data are shown in *Right*. $n = 19$ (WT) or $n = 29$ (LZM) for Ach, $n = 6$ for 8-Br-cGMP. *, $P < 0.05$ vs. WT; **, $P = 0.003$ vs. WT. Open circles, WT; filled circles, LZM. (*C*) Studies of relaxation in cerebrovascular pial (resistance) arteries. Shown is dilation of pressurized pial arteries from WT and LZM mice to the nitric oxide donor SNP. LZM resistance arterial dilation to SNP is markedly impaired compared with WT (*Right*). *, $P < 0.001$. $n = 5$–6 arteries. White bar, WT; black bar, LZM.

mediated relaxation as measured by acetylcholine stimulation of aortic rings with intact endothelium (*SI Text* and Fig. 3*A*). LZM aortic rings also had impaired endothelium-independent relaxation when 8Br-cGMP was used to directly activate PKGI (Fig. 3*B*). Resistance arteries were examined in WT and LZM mice by using *ex vivo* studies of pressurized cerebrovascular pial arteries (28) (*SI Text*). Resistance-sized arteries constrict to an elevation in intravascular pressure ("myogenic tone"). Posterior cerebral pial arteries from both WT and LZM mice were morphologically normal and constricted to 80 mmHg to a similar extent (WT, 22.6 ± 2.5%, $n = 5$; LZM, 25.2 ± 1.6%). To minimize endogenous nitric oxide production, L-NNA (200 μM) was applied, which constricted WT and LZM similarly (by 35.9 ± 4.0% and 33.6 ± 3.6%, respectively) (*SI Text*). As expected, the nitric oxide donor *S*-nitroprusside (SNP) dilated WT by 80.7 ± 6.0%. However, SNP had only a small effect (12.0 ± 5.0%) on arteries from LZM mice (Fig. 3*C*), showing a significant loss of relaxation in LZM vessels in comparison with WT vessels in response to the nitrovasodilator.

Blood pressure was measured in WT and LZM mice (*SI Text*). Significant, sustained elevations in systolic, diastolic, and mean arterial blood pressure (MAP) were evident in 6- to 8-month-old male LZM mice [WT vs. LZM systolic pressure: 113 ± 16 vs. 143 ± 15 mmHg; WT vs. LZM diastolic pressure: 80 ± 19 vs. 101 ± 20 mmHg; WT vs. LZM MAP: 91 ± 18 vs. 115 ± 18 mmHg (mean ± SD)] (Fig. 4 *Left*). Ambulatory telemetric monitoring

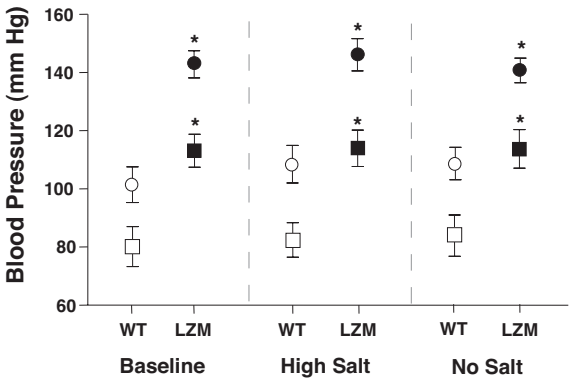

Fig. 4. Blood pressure in LZM and WT mice on normal-salt and altered-salt diets. LZM mice display significant increases in systolic and diastolic blood pressure compared with WT mice. Blood pressures in WT and LZM mice measured in conscious 6- to 8-month-old male mice on normal (0.49% NaCl on the left), high salt (6% NaCl in the center), and salt-deficient (on the right) diets. Blood pressures were measured after 1 week of equilibration on each diet, with 1 week of washout between dietary changes. Systolic (circles) and diastolic (squares) blood pressures are shown for WT (open symbols) and LZM (filled symbols) mice for each dietary sodium condition. $n = 10$ WT and 11 LZM; *, $P < 0.01$ for systolic, mean arterial pressure (MAP) LZM vs. WT (not shown), $P < 0.05$ for diastolic LZM vs. WT, and not statistically significant for systolic, diastolic, and MAP for both genotypes between different salt diets.

studies (*SI Text*) showed that heart rates did not differ between the WT and LZM mice (WT = 538 ± 3, LZM = 544 ± 3, not statistically significant) and confirmed the presence of sustained hypertension in LZM mice of both genders at this age (Fig. S5*A*, Tables S2 and S3, and *SI Text*). Sequential studies of younger mice from 5–14 weeks of age showed that hypertension developed by 10–12 weeks of age in the homozygous LZM mice, whereas heterozygous mice were normotensive (Fig. S5*B*). To examine the possibility that the LZ mutation altered renal function as an explanation for the abnormalities in blood pressure noted, the same group of 6- to 8-month-old male LZM mice and their WT littermates used for the blood pressure studies above were subjected to salt-loading and salt-deprivation studies and renal function studies (*SI Text*). Neither high-salt nor salt-free diets altered the degree of blood pressure elevation noted in the original LZM mice in comparison with WT littermates (Fig. 4 *Center* and *Right*). PKGI is not expressed in renal parenchyma (11, 12), but PKGII inhibits renin secretion and adrenal aldosterone production (13). However, the level of renal expression of PKGII in LZM and WT kidneys was identical (Fig. S6), and circulating aldosterone levels were low and not significantly different in the WT and PKGIα LZM mice (Table 1). Direct measurements of renal glomerular filtration rate (GFR) were made in intact mice using the inulin clearance method (*SI Text*) in the same individual LZM mice and WT littermates from the dietary salt studies above (Fig. 4). No differences in GFR were noted between the two genotypes (LZM GFR = 12.1 ± 1.2 ml/min per kilogram, WT GFR = 10.6 ± 0.7 ml/min per kilogram, not statistically significant) (*SI Text*). Direct measurements of renal plasma flow made by using the paraaminohippuric acid clearance method also did not differ between WT and LZM mice (*SI Text*), nor did the concentrations of BUN, creatinine, or serum electrolytes (Table 1). Other serum studies also did not differ (Tables S4 and S5). Together, these data support that the LZM mice have normal renal function and make unlikely renal dysfunction as a cause of the observed hypertension.

To evaluate the reproducibility of the heritable blood pressure phenotype in multiple mouse lines, the PKGIα LZ mutant mouse was recreated *de novo* on a C57Bl6 background as well as on an SV129 genetic background. Hypertension was again noted in the second C57/bl6 background LZM mouse line created (males, WT vs. LZM systolic = 119 ± 4 vs. 145 ± 8 mmHg, $P = 0.009$; WT vs. LZM diastolic = 88 ± 12 vs. 112 ± 8 mmHg, $P = 0.018$; $n = 10$) and in the newly created SV129 LZM mice (males, WT vs. LZM systolic = 131 ± 4 vs. 143 ± 3 mmHg, $P = 0.019$; WT vs. LZM diastolic = 97 ± 3 vs. 104 ± 2 mmHg, $P = 0.081$; WT vs. LZM MAP = 108 ± 3 vs. 117 ± 3 mmHg, $P = 0.043$) (for females see Table S3) (*SI Text*). Together, these data support that the hypertension observed results from the mutation in the LZ protein interaction domain of PKGIα and the accompanying abnormalities of VSMC and vascular contractile function that result from this mutation.

Discussion

The studies described here demonstrate the importance of PKGIα and its N-terminal LZ targeting domain in maintaining the normal physiology of VSMC and blood vessel tone. The widespread abnormalities of VSMC biology and vascular function seen in the LZM PKGIα mice support that a basal degree of PKGIα activity is required for the maintenance *in vivo* of VSMC plasticity and resting cellular tone. The most striking finding in the PKGIα LZM mice is the presence of elevated blood pressures in the setting of normal renal function and normal renal salt handing, which supports that monogenic molecular abnormalities that directly alter vascular smooth muscle contractile function are sufficient to cause systemic hypertension (6). Hypertension is widely believed to arise exclusively from abnormalities of renal sodium handling (4, 29). Although genetic causes of abnormal blood pressure identified to date largely support this concept (29), these were discovered in genetic studies of early-onset hypertension or hypotension inherited in classic Mendelian patterns, and the cause(s) of hypertension remain unexplained in the large majority (>90–95%) of humans with the disease. Abnormal elevation in vascular smooth muscle tone could produce hypertension by altering systemic vascular resistance and/or renal perfusion (6), although the normal renal function studies described in the LZM mice in this case make the latter explanation less likely. The present study shows that PKGIα regulates normal VSMC phenotype, vascular physiology, and blood pressure via basal control of key VSMC contractile apparatus proteins, including myosin phosphatase and RhoA/Rho kinase. The possibility that high blood pressure can arise from a primary abnormality of vascular smooth muscle function suggests new approaches to the diag-

Table 1. Serum chemistries and aldosterone levels in LZM and WT mice

Mice	Albumin, g/dl	Total protein, g/dl	BUN, mg/dl	Creatinine, mg/dl	Calcium, mg/dl	Phosphorus, mg/dl	Sodium, mEq/liter	Chloride, mEq/dl	Potassium, mEq/liter	Bicarbonate, mEq/liter	Aldosterone, pg/ml
LZM	2.9 ± 0.1	5.2 ± 0.1	22.0 ± 1.1	0.7 ± 0.1	9.3 ± 0.1	5.9 ± 0.2	127.7 ± 8.8	82.2 ± 9.7	3.4 ± 0.5	8.3 ± 0.7	268 ± 65
WT	3.1 ± 0.1	5.4 ± 0.1	25.6 ± 1.7	0.6 ± 0.1	9.4 ± 0.1	7.1 ± 0.5	135.4 ± 3.2	101.2 ± 3.0	3.7 ± 0.3	9.2 ± 1.4	179 ± 77

Data are expressed as mean ± SEM. $n = 5$ mice for LZM and WT for all values except aldosterone ($n = 6$). Differences are not statistically significant for comparison of each parameter between LZM and WT. For additional serum studies, see Tables S4 and S5.

nosis and therapy of a broad range of blood pressure disorders and cardiovascular diseases.

Materials and Methods

Detailed materials and methods, with accompanying supporting figures, may be found in the SI.

ES Cells. Phage clones spanning exon1α of PKG1α were isolated from a mouse 129 genomic library (Stratagene) and used to construct a targeting vector according to standard procedures. All PCR product incorporated in the final targeting vector was verified by bidirectional sequencing. Conditions for growth and electroporation of CCE embryonic stem cells, G418 selection, and preparation of chimeric mice were as described (30).

Animal Care and Naming. Throughout the studies described herein, animal care was in accordance with and approved by the Institutional Animal Care and Use Committee of Tufts University School of Medicine. The first LZM mouse line created is referred to as the ''original'' LZM colony, and all studies in this article were done with these unless otherwise noted. Two additional mouse LZM lines were created in 2005 and 2006 by introduction of targeted SV129 ES cells into both C57Bl6 blastocysts (LZM06 C57Bl6) and SV129 blastocysts (LZM06 SV129). These two lines were used to evaluate the reproducibility of the heritable blood pressure phenotype in multiple mouse lines, as described in this article.

RT-PCR. RT-PCR was done in standard fashion, as described in *SI Text*.

Purification of GST Fusion Proteins, Immunoblotting, and GST Pull-Down Experiments. All were expressed and purified in standard fashion, as described previously (17, 25) and in *SI Text*. Protein lysates were made from WT and LZM VSMCs in culture as described (31).

RhoA Activity and RhoA-S188-PO_4. For RhoA activation, GTP-bound RhoA was measured by using GST-Rhotekin-RBD binding assays as described (32). For determination of RhoA-S188-PO_4, WT and LZM VSMC lysates were resolved by SDS/PAGE and immunoblotted with anti-RhoA-S188-PO_4 antibodies in standard fashion, as described in *SI Text*.

PKGI Kinase Assay. PKGI kinase assays were done in standard fashion, as described in *SI Text*, using a specific substrate for PKG (33).

PKG-II Expression in the Kidneys in WT and LZM Mice. Kidney lysates from WT and LZM mice were prepared and immunoblotted with anti-PKG-II antibodies in standard fashion, as described in *SI Text*.

Electrophysiological Recordings from WT and LZM VSMC. Isolation of single smooth muscle cells from cerebral arteries was as reported (7) and as described in *SI Text*. Patch clamp recordings from isolated myocytes from cerebral arteries were done in standard fashion, as described in *SI Text*.

***In Vivo* Stress Fiber Staining.** Aortic endothelium was analyzed as described (8) (for details see *SI Text*).

VSMC Morphology and Immunofluorescence. Explant and enzymatic preparations of primary, unpassaged VSMC were made as described previously (9), and VSMC morphology and immunofluorescence staining was performed (for details see *SI Text*).

Murine Vascular Ring Studies. Vascular ring studies were performed with mouse thoracic aortic rings as described previously (25) (for details see *SI Text*).

Isolated Resistance Arterial Preparation. Posterior cerebral arteries were isolated, cannulated, and mounted in an arteriograph for measurement of arterial diameters (for details see *SI Text*).

Telemetric Blood Pressure Measurements. Telemetric blood pressure measurements were made in ambulatory mice using implantable, miniaturized mouse blood pressure transmitters as described (25).

Tail-Cuff Blood Pressure Measurements. Systolic, diastolic, and mean blood pressures of conscious 6- to 12-month-old mice were measured by using a tail cuff blood pressure analyzer designed with volume-pressure recording technology (for details see *SI Text*).

Renal Function Assays. Inulin clearance is used as a measure of GFR, and paraaminohippuric acid (PAH) clearance is used as an estimate of renal plasma flow. Clearances of inulin and PAH were measured as described by Coffman and coworkers (refs. 11 and 12 in *SI Text*).

Statistical Methods. All data are shown as mean $\pm$ SE except where noted as $\pm$ SD. For pairwise analysis, Student's *t* tests were used. Multiple group comparisons were made by one-way or two-way ANOVA, as appropriate. For significant between-group differences found by ANOVA, multiple pairwise comparisons were made with the Student–Newman–Keuls method. For all statistical comparisons, $P < 0.05$ was considered significant.

ACKNOWLEDGMENTS. We thank Liz Robertson (Harvard University, Cambridge, MA) for ES cells, Kirk Thomas (University of Utah, Salt Lake City, UT) for the protamine Cre cassette, Kemp Herzburg and Elisa Abdulhayoglu1for technical assistance with creating the LZM mice, and Ping Lu for technical help with vascular ring studies. We are grateful to Tom Coffman and Susan Gurley from Duke University for generous help and guidance with all aspects of the renal studies. This work was supported in part by National Institutes of Health Grants PO1 HL077378 and HL55309 (to M.E.M.), by National Institutes of Health Grants HL44455 and HL63722 (to M.T.N.), and by National Institutes of Health Postdoctoral Trainee Fellowship HL07944 (to M.K.W.).

1. Kannel WB (2000) Elevated systolic blood pressure as a cardiovascular risk factor. *Am J Cardiol* 85:251–255.
2. Somlyo AP, Somlyo AV (1994) Signal transduction and regulation in smooth muscle. *Nature* 372:231–236.
3. Davis MJ, Hill MA (1999) Signaling mechanisms underlying the vascular myogenic response. *Physiol Rev* 79:387–423.
4. Guyton AC, *et al.* (1972) Arterial pressure regulation. Overriding dominance of the kidneys in long-term regulation and in hypertension. *Am J Med* 52:584–594.
5. Touyz RM (2000) Molecular and cellular mechanisms regulating vascular function and structure—implications in the pathogenesis of hypertension. *Can J Cardiol* 16:1137–1146.
6. Mendelsohn ME (2005) In hypertension, the kidney is not always the heart of the matter. *J Clin Invest* 115:840–844.
7. Uehata M, *et al.* (1997) Calcium sensitization of smooth muscle mediated by a Rho-associated protein kinase in hypertension. *Nature* 389:990–994.
8. Lincoln TM (1994) *Cyclic GMP: Biochemistry, Physiology and Pathophysiology* (R.G. Landes, Austin, TX).
9. Murad F (2006) Nitric oxide and cyclic GMP in cell signaling and drug development. *N Engl J Med* 355:2003–2011.
10. Hofmann F (2005) The biology of cyclic GMP-dependent protein kinases. *J Biol Chem* 280:1–4.
11. Joyce NC, DeCamilli P, Lohmann SM, Walter U (1986) cGMP-dependent protein kinase is present in high concentrations in contractile cells of the kidney vasculature. *J Cyclic Nucleotide Protein Phosphor Res* 11:191–198.
12. Gambaryan S, *et al.* (1998) Endogenous or overexpressed cGMP-dependent protein kinases inhibit cAMP-dependent renin release from rat isolated perfused kidney, microdissected glomeruli, and isolated juxtaglomerular cells. *Proc Natl Acad Sci USA* 95:9003–9008.
13. Wagner C, Pfeifer A, Ruth P, Hofmann F, Kurtz A (1998) Role of cGMP-kinase II in the control of renin secretion and renin expression. *J Clin Invest* 102:1576–1582.
14. Hofmann F, Feil R, Kleppisch T, Schlossmann J (2006) Function of cGMP-dependent protein kinases as revealed by gene deletion. *Physiol Rev* 86:1–23.
15. Gambaryan S, *et al.* (2003) cGMP-dependent protein kinase type II regulates basal level of aldosterone production by zona glomerulosa cells without increasing expression of the steroidogenic acute regulatory protein gene. *J Biol Chem* 278:29640–29648.
16. Ignarro LJ, Kadowitz PJ (1985) The pharmacological and physiological role of cyclic GMP in vascular smooth muscle relaxation. *Annu Rev Pharmacol Toxicol* 25:171–191.
17. Surks HK, *et al.* (1999) Regulation of myosin phosphatase by a specific interaction with cGMP-dependent protein kinase Ia. *Science* 286:1583–1587.
18. Somlyo AP, Somlyo AV (2000) Signal transduction by G-proteins, Rho-kinase and protein phosphatase to smooth muscle and non-muscle myosin II. *J Physiol* 522:177–185.
19. Fukata Y, Amano M, Kaibuchi K (2001) Rho-Rho-kinase pathway in smooth muscle contraction and cytoskeletal reorganization of non-muscle cells. *Trends Pharmacol Sci* 22:32–39.
20. Sauzeau V, *et al.* (2000) Cyclic GMP-dependent protein kinase signaling pathway inhibits RhoA-induced Ca2+ sensitization of contraction in vascular smooth muscle. *J Biol Chem* 275:21722–21729.
21. Sauzeau V, Rolli-Derkinderen M, Marionneau C, Loirand G, Pacaud P (2003) RhoA expression is controlled by nitric oxide through cGMP-dependent protein kinase activation. *J Biol Chem* 278:9472–9480.
22. Orstavik S, Natarajan V, Taskén K, Jahnsen T, Sandberg M (1997) Characterization of the human gene encoding the type Ia and type Ib cGMP-dependent protein kinase (PRKG1). *Genomics* 42:311–318.

23. Feil R, Lohmann SM, de Jonge H, Walter U, Hofmann F (2003) Cyclic GMP-dependent protein kinases and the cardiovascular system: Insights from genetically modified mice. *Circ Res* 93:907–916.
24. Geiselhoringer A, *et al.* (2004) IRAG is essential for relaxation of receptor-triggered smooth muscle contraction by cGMP kinase. *EMBO J* 23:4222–4231.
25. Tang M, *et al.* (2003) Regulator of G-protein signaling 2 mediates vascular smooth muscle relaxation and blood pressure. *Nat Med* 9:1506–1512.
26. Surks, Howard K, Mendelsohn, Michael E (2003) Dimerization of cGMP-dependent protein kinase 1α and the myosin-binding subunit of myosin phosphatase: Role of leucine zipper domains. *Cell Signalling* 15:937–944.
27. Ridley AJ, Hall A (1992) The small GTP-binding protein rho regulates the assembly of focal adhesions and actin stress fibers in response to growth factors. *Cell* 70:389–399.
28. Gonzalez Bosc LV, *et al.* (2004) Intraluminal pressure is a stimulus for NFATc3 nuclear accumulation. *J Biol Chem* 279:10702–10709.
29. Lifton RP, Gharavi AG, Geller DS (2001) Molecular mechanisms of human hypertension. *Cell* 104:545–556.
30. Michael SK, Brennan J, Robertson EJ (1999) Efficient gene-specific expression of Cre recombinase in the mouse embryo by targeted insertion of a novel IRES-Cre cassette into endogenous loci. *Mech Dev* 85:35–47.
31. Surks H, Richards CT, Mendelsohn ME (2003) Myosin phosphatase-Rho interacting protein: A new member of the myosin phosphatase complex that directly binds RhoA. *J Biol Chem* 278:51484–51493.
32. Surks HK, Riddick N, Ohtani K (2005) M-RIP targets myosin phosphatase to stress fibers to regulate myosin light chain phosphorylation in vascular smooth muscle cells. *J Biol Chem* 280:42543–42551.
33. Colbran JL, *et al.* (1992) A phenylalanine in peptide substrates provides for selectivity between cGMP- and cAMP-dependent protein kinases. *J Biol Chem* 267:9589–9594.
34. Sakurada S, Okamoto H, Takuwa N, Sugimoto N, Takuwa Y (2001) Rho activation in excitatory agonist-stimulated vascular smooth muscle. *Am J Physiol* 281:C571–C578.